IOP Conf. Series: Materials Science and Engineering **408** (2018) 012013 doi:10.1088/1757-899X/408/1/012013

Numerical Study of the Circumferential Fluctuations in Swept Compressor Cascades

Zefeng Li[1,2], Lei Wen[3], Mingzhi Tang[4], Donghai Jin[1,5,*] and Xingmin Gui[1,5]

[1]School of Energy and Power Engineering, Beihang University, Beijing, China
[2]Shen Yuan Honors College of Beihang University, Beijing, China
[3]Technical Division, Shanghai Electric Gas Turbine Co., Ltd, Shanghai, China
[4]AECC Shenyang Engine Research Institute, Shenyang, China
[5]Collaborative Innovation Center of Advanced Aero-Engine, Beijing, China

[*]jdh@buaa.edu.cn

Abstract. This paper presents comparative numerical studies to analyze the inlet flow and circumferential fluctuation(CF) source terms in compressor cascades. Forward swept cascades with different sweep angles and straight cascade were calculated numerically by a computational fluid dynamics(CFD) package to get the required three-dimensional(3D) flow parameters. A dimension reduction method was introduced and an in-house code for data reduction was conducted to obtain a circumferentially averaged flow field. The results show that different sweep angle and nominal incidence angle will change the magnitude and distribution of the CF source terms at inlet thus altering the inlet flow field. The Mach number(Ma) could also change the inlet CF source terms under the same swept angle. The trends of radial migration and the blade loading would increase with the growing of the inlet Ma.

1. Introduction

In recent years, the developing trend of aeroengine fans/compressors concentrates on high through-flow, high efficiency, high loading, and acceptable stability operation margin. Swept blades techniques are widely explored in the aerodynamic design of axial fans/compressors to meet the above requirements effectively. However, due to the complexity of 3D viscous flow field of swept blade, the mechanism of sweep has not been fully understood yet.

Lots of researches of the impact of the sweep blade on flow field have been carried out by former researchers recently. Wennerstrom and Frost[1] firstly introduce sweep design in a highly loaded transonic fan in the HTFC program in 1976. Wadia[2] applied the forward sweep rotor to multi-stage fans and found that the structure of sweep blades can improve the sensitivity of compressors to inlet distortion. McNulty[3] suggested that forward swept rotor could induce higher inlet axial velocity at blade tip and lower at blade hub. Sweep can lead to a spanwise redistribution of flow with more flow to the tip sections. The authors further concluded that forward sweep reduced tip-leakage flow blockage and tip loading.

Passrucker[4] utilized forward sweep technique in rotor design of a transonic compressor and experimental results show that forward sweep rotor possesses a higher efficiency and wider stall margin. Forward sweep could induce the flow to the blade tip, especially at the near-stall operation

state, which contributes to the flow stability in the tip region. Rotor with sweep can work stably although separation happened around the hub.

Zhu Fang[5] reduced the dimension of inviscid momentum equations of compressors for analysis and suggested that the circumferential fluctuation of pressure field in the blade passage affected the flow in the form of inviscid blade force in 2013. The influence of the inviscid blade force will extend to the upstream and lead to the inlet CF of the flow field. They also suggested that the effect of forward sweep is opposite to backward sweep. Chang Hao investigated the inlet radial equilibrium from the aspect of circumferential averaging and found that the most important terms in the radial equilibrium are the GPR, and CMR. They also explained the inlet flow field alteration related to the aerodynamic behaviour of swept blades. Chang analyzed the effect of blade sweep on the inlet radial equilibrium of cascades.[6]

Tang proposed a transport model for the CF source terms[7] induced by inviscid blade force at the inlet of the blade to include more 3D effects in the circumferential averaged throughflow model in 2016. With the CF terms included, a major enhancement in the prediction capability of the throughflow analysis is obtained.

An objective of this study was to further investigate the mechanism of sweep blade. In this paper, comparative compressor cascades were studied numerically to analyze the impact of blade sweep on the CF and the flow field. The circumferential average method is generally averaged in arc direction of annular cascades and the circumferential average in this paper is particularly along the pitch direction.

2. Circumferentially averaged momentum equations

2.1. The coordinates for cascades

The Coordinates for the cascades in this paper is regulated as figure 1, where coordinate x is axial direction, y stands for circumferential direction and coordinate z is the radial direction respectively.

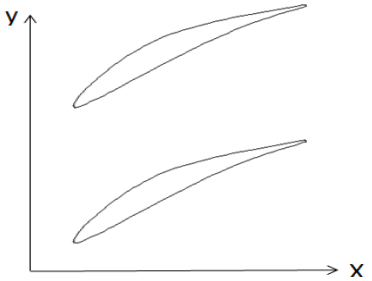

Figure 1. The coordinates set for cascades

2.2. Circumferential average method

The circumferentially averaging operation is defined as follows:

$$\bar{q}(x,z,t)=\frac{1}{y_p-y_s}\int_{y_s}^{y_p} q(x,y,z,t)dy \tag{1}$$

Where $\bar{q}$ is the circumferential averaged value of q, y_p-y_s the pitch length of the blade passage and the subscript p, s stand for the pressure side (PS)and suction side(SS) respectively. With the definition of circumferential averaging, the 3D flow parameter can be decomposed into the sum of a circumferential averaged term and a spatial fluctuation which reflects the circumferential non-uniformity of the flow field. It can be expressed as:

$$q(x,y,z,t)=\bar{q}(x,z,t)+q'(x,y,z,t) \tag{2}$$

Due to the non-linearity of the equations, the fluctuations appear in the form of the circumferentially averaged stresses, i.e. the so-called CF stresses[7], which cannot be eliminated in the

governing equation after circumferential dimension reduction like Reynold Stress. The non-linear terms in incompressible flow can be expressed as equation (3) and equation (4) state.

$$\overline{q_1 q_2} = \overline{q}_1 \overline{q}_2 + \overline{q'_1 q'_2} \tag{3}$$

$$\overline{\rho q_1 q_2} = \rho(\overline{q}_1 \overline{q}_2 + \overline{q'_1 q'_2}) \tag{4}$$

2.3. The momentum equations

The Navier–Stokes (N–S) momentum equation in Cartesian coordinates can be expressed in the axial, radial and circumferential direction, with volume force and viscous term neglected and steady assumption, as follows:

$$\begin{cases} \frac{\partial}{\partial x}(\rho u^2 + p) + \frac{\partial}{\partial y}(\rho uw) + \frac{\partial}{\partial y}(\rho uv) = 0 \\ \frac{\partial}{\partial x}(\rho uw) + \frac{\partial}{\partial y}(\rho w^2 + p) + \frac{\partial}{\partial y}(\rho wv) = 0 \\ \frac{\partial}{\partial x}(\rho uv) + \frac{\partial}{\partial y}(\rho vw) + \frac{\partial}{\partial y}(\rho v^2 + p) = 0 \end{cases} \tag{5}$$

Where ρ is the density, p the pressure and u, v, w represent the axial, circumferential and radial velocity respectively. Employing the circumferential averaging operator equation (1) to equation (5) yields

$$\begin{cases} \frac{\partial}{\partial x}(\bar{u}\,\bar{u}) + \frac{\partial}{\partial z}(\bar{w}\,\bar{u}) = -\frac{1}{\rho}\frac{\partial \bar{p}}{\partial x} + P_x + F_{bx} \\ \frac{\partial}{\partial x}(\bar{u}\,\bar{v}) + \frac{\partial}{\partial z}(\bar{w}\,\bar{v}) = P_y + F_{by} \\ \frac{\partial}{\partial x}(\bar{w}\,\bar{u}) + \frac{\partial}{\partial z}(\bar{w}\,\bar{w}) = -\frac{1}{\rho}\frac{\partial \bar{p}}{\partial z} + P_z + F_{bz} \end{cases} \tag{6}$$

where

$$\begin{cases} P_x = -\frac{1}{b}\frac{\partial}{\partial x}\left(b\overline{u'u'}\right) - \frac{1}{b}\frac{\partial}{\partial z}\left(b\overline{u'v'}\right) \\ P_y = -\frac{1}{b}\frac{\partial}{\partial x}\left(b\overline{u'w'}\right) - \frac{1}{b}\frac{\partial}{\partial z}\left(b\overline{v'w'}\right) \\ P_z = -\frac{1}{b}\frac{\partial}{\partial x}\left(b\overline{u'v'}\right) - \frac{1}{b}\frac{\partial}{\partial z}\left(b\overline{v'v'}\right) \end{cases} \tag{7}$$

and

$$\begin{cases} F_{bx} = \frac{N}{\rho l b}\left(P_p \frac{\partial y_p}{\partial x} - P_s \frac{\partial y_s}{\partial x}\right) \\ F_{by} = \frac{N}{\rho l b}\left(P_s - P_p\right) \\ F_{bz} = \frac{N}{\rho l b}\left(P_p \frac{\partial y_p}{\partial z} - P_s \frac{\partial y_s}{\partial z}\right) \end{cases} \tag{8}$$

F_b is the inviscid blade force, $\overline{u'u'}$, $\overline{v'v'}$, $\overline{w'w'}$, $\overline{u'v'}$, $\overline{u'w'}$, $\overline{v'w'}$ are the CF stresses terms and they are symbolled as UU,VV,WW,UV,UW,VW respectively in this paper. CF stresses terms are related to the blade-to-blade spatial fluctuations[7], arising in the circumferential averaging of the 3D N-S equations, due to the non-linearity of the equations. P is the CF source term and b is the blockage factor that represents circumferential blade thickness distribution, which is calculated as equation (9):

$$b = \frac{y_P - y_S}{l / N} \tag{9}$$

Where l refers to the circumferential length of the blade passage and N represents the number of blades. The blockage factor b is less than 1.0 within blade area and equal to 1.0 outside.

3. Computational Methodology

3.1. Definition of sweep

Different definitions of sweep have been adopted in the literatures. In this paper, the definition of sweep defined by Ramakrishna and Govardhan[8] is used. The sweep was defined as moving airfoil sections along the chord line (see figure 2 and Θ is the blade camber angle). According to Denton and Xu[9], defining sweep in this way would not introduce any spanwise blade force, whereas lean (moving the blade sections perpendicular to the chord line) would introduce the influences of spanwise blade forces.

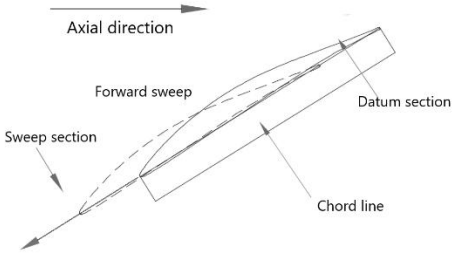

Figure 2. The definition of Sweep

The sweep angle was defined as the angle between the leading edge of the cascade and the radial direction in a radial profile section. When a higher span section was moved in the upstream direction relative to the lower section, it is defined as forward sweep. In this paper, the sweep angle keeps the same alongside all the spanwise profile sections to focus on the mechanism of sweep impact on the inlet flow.

3.2. Cascade model

The blade profile is identical at all spanwise sections in every cascade to ensure a concentrative study on the mechanism of blade sweep. A circular arc was adopted for the style of blade airfoil camber. The thickness distribution is the same as the MAN GHH 1-S1 controlled diffusion airfoil[10] and other specific parameters are listed in Table 1

Table 1. Three Scheme comparing.

Parameter	Value
Blade camber angle θ / °	30
Chord length/mm	50
Blade geometric inlet angle β_{1k} / °	57
Aspect ratio	2.4
Pitch length/mm	33

3.3. CFD method

NUMECA FINE/Turbo was used to carry out numerical simulation for 3D flow field of cascades in this paper. The mesh was drawn with around 429,135 grid points and a selected O4H topology, which is shown in Figure 3.

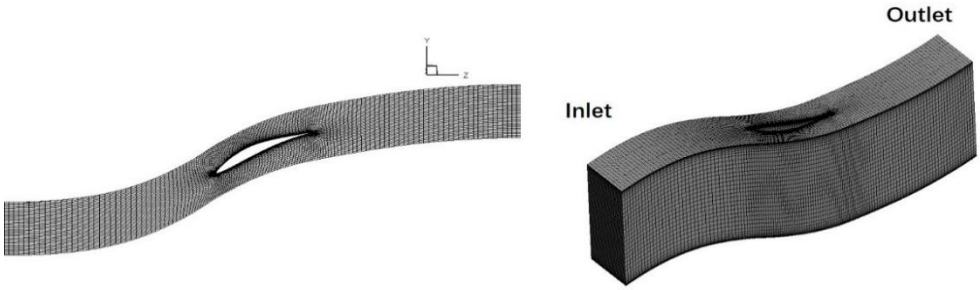

Figure 3. View of grid of computational domain

The length of the inlet and outlet domain were set to 2 times as long as the chord line. For turbulence calculation, the Spalart–Allmaras model was selected for calculation. The boundary condition was the total pressure(101325Pa), total temperature(277.15K) and direction of flow fixed at the inlet and the static pressure set at the outlet to ensure an inlet Mach number(Ma), adiabatic non-slipping condition was used for solid wall boundaries. In this study, only one cascade passage was modeled to save computational resource and periodical continuous boundary was set to ensure the repeatability of cascades.

4. Results and discussion

The circumferential fluctuation can be caused by many aspects, including the inhomogeneity of the incoming flow, the trail of upstream blade row, tip leakage, vortex, passage shock, shock-boundary layer interaction, hub corner stall and the pressure fluctuation in the blade passage[11], as well as the inviscid blade force[12]. For cascades, the main factor responsible for the inlet flow CF is the circumferential pressure fluctuation (inherent characteristic of the flow field of non-axisymmetric geometry) inside the cascade passages as the upstream flow was set to uniform. The influence of such pressure CF would extend to the upstream to a distance from the leading edge thus inducing the inlet circumferential fluctuations. A program for circumferential data reduction was developed to get the required variables to calculate the CF source terms, CF stress terms and other flow parameters.

4.1. Influence of blade sweep

Figure Figure **4** plots the axial distribution of the CF stresses terms at the mid-span section in straight cascade. The relative axial location is defined as the distance from the leading edge normalized by the chord length. 0 location stands for the leading edge(LE) and 100% represents the trailing edge(TE).

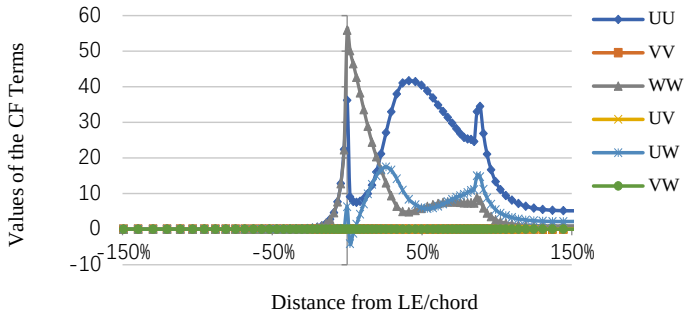

Figure 4. Axial distribution of CF stresses at mid-span in straight cascade

For straight cascades, the radial component of the inviscid blade force is 0 and the radial velocity is close to 0, which means that the CF stresses terms (VV, UV, VW) related to radial velocity V are approached to 0. However, the other CF stresses term (UU, UW, WW) are not ignorable at the location before the leading edge and the axial gradients of these terms are large, the axisymmetric assumption may fail to obtain an acceptable flow field in throughflow model[7].

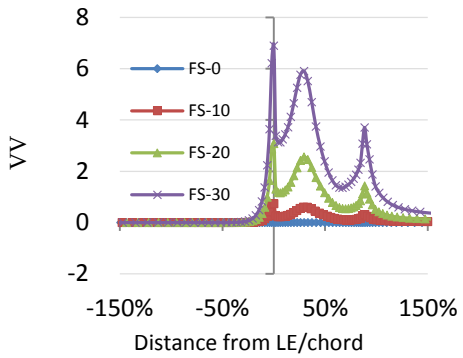

Figure 5. Axial Distribution of VV in different cascades at 50% spanwise

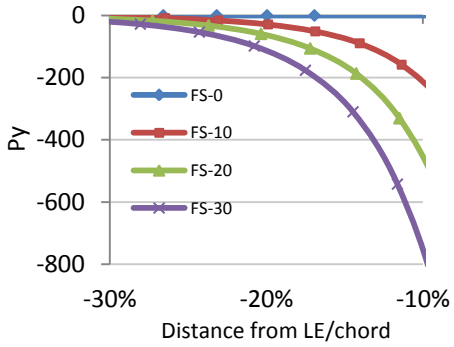

Figure 6. Axial distribution of Py in different cascades at 50% spanwise

To study the sweep effect on CF of the flow field, 3 different forward sweep angle 10 º, 20 ºand 30 ºwere calculated respectively. FS-0 stands for the straight blade and the sweep blade are similarly named. From Figure 5 and Figure 6, the VV term and the circumferential component of CF source term P_y increase with the growing of sweep angle, which indicate that the sweep induces the CF in the flow fields. The gradient of VV increases with growing sweep angle before the LE, which also reflect the intensifying of CF.

4.2. Influence of nominal incidence angle

Nominal incidence angle in defined as the domain inlet flow angle minus the blade geometrical inlet angle β_{1k}, which reflects the free inlet flow direction relative to the cascade geometrical inlet angle. The spanwise distribution of the CF source term P_y at 4% chord length before LE for straight cascades with nominal incidence angle equal to 0 º, ±2 ºand ±4 ºis shown in Figure 7.

The regions below 40% of the span and above 60% of the span are omitted, due to the viscous and end-wall effect. It indicates that the magnitude of P_y increases with the growing of incidence angles, which can reflect the blade loading. Bigger magnitude of P_y means bigger pressure difference between pressure surface and suction surface, as Figure 8 illustrates.

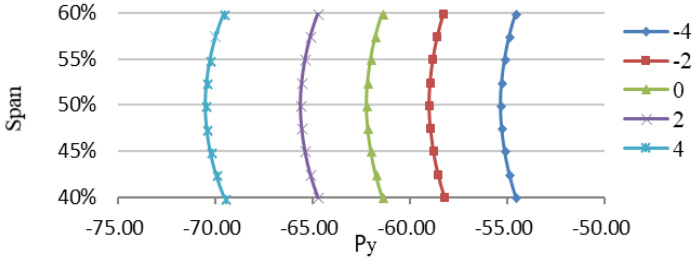

Figure 7. Spanwise Distribution of P_y at 4% chord before LE with different nominal incidence angle.

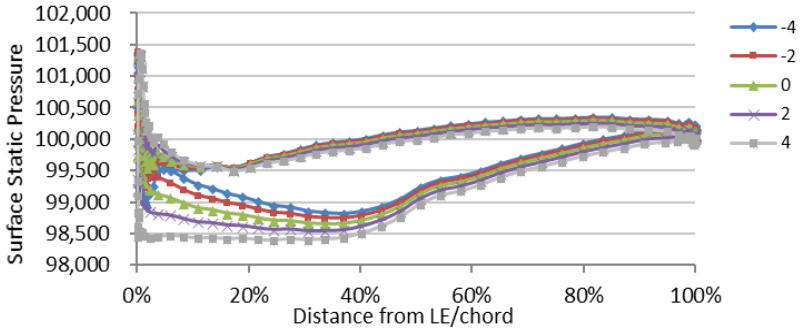

Figure 8. Pressure Distribution on blade surface at mid-span

4.3. Comparison of different Mach Number

In multi-stage compressors, the different spanwise sections of a blade row often work under different inlet velocity, thus we want to study the influence of the Mach number on the inlet CF. 30 ° forward sweep cascade was calculated under inlet Ma equal to 0.15, 0.2 and 0.25, the nominal incidence angle for all cases in this subsection are 0 °.

As the CF source terms are relevant to velocities, it is nondimensionalized as equation (10) to investigate the variation of CF under different inlet velocity.

$$P' = -\frac{P}{V_{in}^{2}}\mathrm{h} \tag{10}$$

Where P' is the dimensionless CF source term, V_{in} the absolute velocity at the mid-span on the inlet and h is the span length.

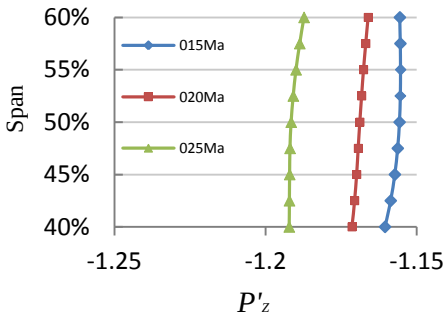

Figure 9. Spanwise Distribution of P'_z at 4% chord before LE with different Ma

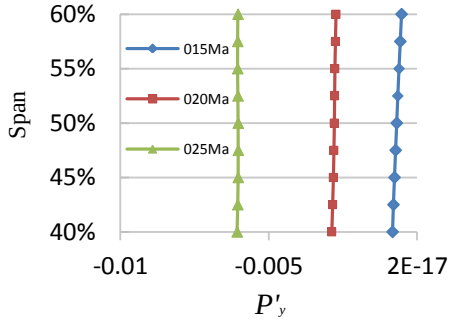

Figure 10. Spanwise Distribution of P'_y at 4% chord before LE with different Ma

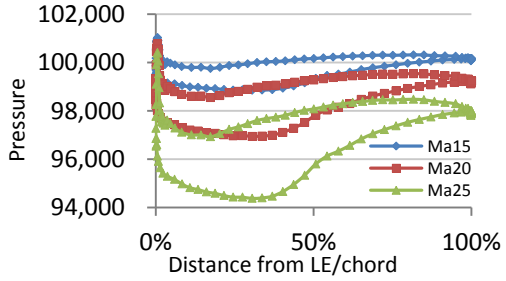

Figure 11. Axial pressure distribution with different Ma

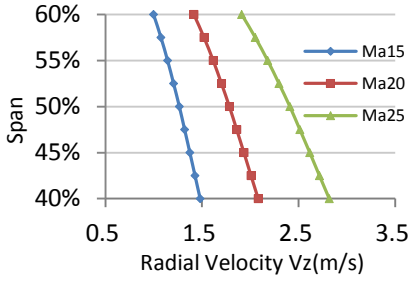

Figure 12. Spanwise Distribution of Vz at 4% chord before LE with different Ma

Figure 9 and 10 state the distribution of the radial and circumferential components of the CF source terms at 4% chord axial location before LE with different Ma. Different Ma cause different acceleration characteristic of blade surface. Higher Ma induce stronger CF, larger blade loading, thus higher pressure difference between PS and SS, which can be reflected in Figure 11. The increase of P'_z alters the inlet radial equilibrium, as is shown in Figure 12 the radial migration is enhanced.

5. Conclusion

Comparative numerical studies have been carried out on cascades to investigate the effect of blade sweep on circumferential fluctuations in axial compressor cascades. Although this work is based on an inviscid and incompressible flow, the flow mechanism is quite accurately calculated as viscous effects are secondary in free stream flows and the Ma is less than 0.3 in all cases.

The magnitude of circumferential components of CF source term P_y and the VV term increase with growing sweep angle. High sweep angle will induce radial migration of the flow from hub to tip. CF

also exists in straight cascade as discussed before, the CF terms related to radial velocity are small in straight cascades due to the low radial velocity.

The inlet incidence angles also affect the CF, bigger magnitude of P_y means bigger difference between pressure surface and suction surface and blade loading.

Under the same sweep angle, as the Mach Number increases, CF and the trend of radial migration of the flow will be intensified. The blade loading will also increase with Ma, so the inlet Ma should be carefully considered in the design process.

References

[1] Wennerstrom A and Frost G 1976 Design of a 1500 ft/sec, transonic,high-through-flow, single-stage axial-flow compressor with low hub/tip ratio Report No: AFARL-TR-76-59
[2] Wadia A, Szucs P and Crall D, et al 2002 Forward Swept Rotor Studies in Multistage Fans with Inlet Distortion *ASME Paper* GT-2002-30326
[3] McNulty G, Khalid S, Decker J, et al 2004 The Impact of Forward Swept Rotors on Tip Clearance Flows in Subsonic Axial Compressors *J. of turbomachinery* **126**(4):445-454
[4] Passrucker H 2003 Effect of Forward Sweep in a Transonic Compressor Rotor *J. of Power and Energy*, **V217**(4): 357-365
[5] ZHU F 2013 Study on design techniques of high through flow and high efficiency fan/booster of civil aeroengine Beijing: Beihang University
[6] Chang H, ZHU F, Jin D and Gui X 2015 Effect of Blade Sweep on Inlet Flow in Axial Compressor Cascades *Chinese Journal of Aeronautics*, **28**(1): 103-111
[7] Tang M, Jin D and Gui X 2017 Modeling and Numerical Investigation of the Inlet Circumferential Fluctuationsof Swept and Bowed Blades *J. of Thermal Science* **26**(1):1-10
[8] Raamakrishna P and Govardhan M 2010 Numerical Study of the Stagger Angle Effects in Forward Swept Axial Compressor Rotor Passages *ASME Turbo Expo 2010: Power for Land, Sea, and Air* pp443-453
[9] Denton J and Xu L 2002 The Effects of Lean and Sweep on Transonic Fan Performance. *ASME Turbo Expo 2002: Power for Land, Sea, and Air.* **6** p23-32
[10] Steinert W, Eisenberg B and Starken H 1991 Design and testing of a controlled diffusion airfoil cascade for industrial axial flow compressor application *J. of Turbomachinery* **4**.1991-10:583-590
[11] Baralon S, Eriksson L and Hall U 1999 Evaluation of Higher-Order Terms in the Throughflow Approximation Using 3D Navier-Stokes Computations of a Transonic Compressor Rotor *ASME 1999 International Gas Turbine and Aeroengine Congress and Exhibition* V**001** T03A013
[12] Gui X, Zhu F and Jin D 2013 Effects of Inlet Circumferential Fluctuation on the Sweep Aerodynamic Performance of Axial Fans/Compressors *Journal of Thermal Science* **22**(5):383-394